Theoretical study on ethene metathesis proceeding on Mo^{VI} and Mo^{IV} methylidene centres of heterogeneous molybdena-alumina catalyst

Jarosław Handzlik*, Jan Ogonowski

Institute of Organic Chemistry and Technology, Cracow University of Technology, ul. Warszawska 24, PL 31-155 Kraków, Poland

Abstract

Theoretical studies on ethene metathesis reaction proceeding on molybdenamethylidene centres of molybdena-alumina catalyst are reported. Calculations were carried out with the Gaussian 94 program, using density functional theory. Models of active sites containing Mo^{VI} and Mo^{IV} (both singlet and triplet state) have been developed. Molybdenum in these centres is attached to a cluster of formula $Al_2(OH)_6$, which represents alumina. The thermodynamics of the reactions of ethene with Mo^{VI} and Mo^{IV} carbene centres were calculated. The reaction pathways of ethene addition to Mo^{VI} and Mo^{IV} methylidene complexes were also investigated. In these calculations simpler structures of the carbene and molybdacyclobutane complexes have been applied, in which the bonds between molybdenum and the carrier are replaced by hydroxyl groups. It was concluded that active centres of ethene metathesis do not contain Mo^{IV} because of high energy barriers of some elementary steps of the process. © 2001 Elsevier Science B.V. All rights reserved.

Keywords: Molybdena-alumina catalyst; Ethene metathesis; DFT; Gaussian

1. Introduction

Olefin metathesis can be carried out in the presence of both homogeneous and heterogeneous catalytic systems [1,2]. The reaction proceeds according to the carbene mechanism [3] and active carbene complexes are present in the reaction environment. Metal carbene reacts with olefin, thus forming the metallacyclobutane complex. Subsequent decomposition of the metallacyclobutane leads to formation of a new olefin and a carbene structure.

Many theoretical investigations of the structures and reactivity of the olefin metathesis catalysts were reported [4–15]. They all concern Mo^{VI} alkylidene complexes playing a role in homogeneous catalysis. Goddard and co-workers [4–6] investigated Cr, Mo and W alkylidene complexes and thermodynamics of their reactions with ethene. The authors applied generalised valence bond method. An ab initio Hartree–Fock study on the structures and electronic properties of metal alkylidene complexes including Mo, W and Re was reported by Cundari and Gordon [7,8]. Bencze and Szilagyi [9–11] applied molecular mechanics in modelling of tungsten catalysts. Addition of ethene to tungsten methylidene complex $W(CH_2)(Cl)_4$ was investigated by Sodupe et al. at the Hartree–Fock level [12]. They localised the ethene-tungsten-methylidene complex, which was thought to be an intermediate in the formation of the metallacyclobutane. Folga and Ziegler [13] applied density functional theory to

* Corresponding author. Tel.: +48-12-6282761;
fax: +48-12-6282037.
E-mail address: jhandz@usk.pk.edu.pl (J. Handzlik).

study the structures of $Mo(X)(CH_2)(L)_2$ alkylidene and $Mo(X)(CH_2CH_2CH_2)(L_2)$ (X = O, NH; L = Cl, OCH_3, OCF_3) molybdacyclobutane complexes. They discussed the reaction path of molybdacyclobutane formation via ethene attack on the CNO face of the alkylidene complex (X = NH). The authors concluded that in the presence of the electron-withdrawing ligands (L = OCF_3) a trigonal-bipyramidal (TBP) molybdacyclobutane is formed. On the other hand, the electron-donating ligands (L = OCH_3) result in the formation of a square-pyramidal (SP) molybdacyclobutane. Schrock and co-workers [14] carried out SCF-X_α-SW calculations on $Mo(NH)(CH_2)(OH)_2$ and $Mo(NH)(CH_2)(OCH_3)_2$ alkylidene complexes and $Mo(NH)(CH_2CH_2CH_2)(OH)_2$ molybdacyclobutane complex. In their work the electronic properties of the complexes were studied and concerted alkylidene rotation and molybdacyclobutane formation via olefin attack on the COO face of the Mo^{VI} imido alkylidene complex was considered. Ab initio and density functional theory study on ethene addition to $Mo(NH)(CHR)(L)_2$ complexes (R = H, CH_3; L = OCH_3, OCF_3) was reported by Wu and Peng [15]. They localised transition structures leading to the formation of TBP molybdacyclobutanes and proved that there is a significant preference for ethene to attack the CNO face over the COO face of the Mo alkylidene complex. They also showed that the calculated activation enthalpy of ethene addition to the complex with OCF_3 ligands is lower than in the case of the addition to the complex possessing OCH_3 ligands. According to their calculations, the TBP geometry of molybdacyclobutane is slightly more stable than the SP geometry if L = OCF_3. If molybdacyclobutane possesses electron-donating ligands (L = OCH_3), the SP geometry is much more stable than the TBP geometry.

On the other hand, theoretical studies on olefin metathesis proceeding on heterogeneous catalysts have not been reported so far. Such investigations could help to answer some questions concerning heterogeneous systems. In contrast with homogeneous catalysts, the structures of active centres of heterogeneous catalysts are usually not well defined. The reason is the fact that the number of active sites of heterogeneous catalysts is only a small fraction of the amount of transition metal atoms on the surface [1,2]. In the case of the active sites of heterogeneous molybdena catalysts, Mo valence is not ultimately proved.

There are many experimental evidences that the surface alkylidene centres contain Mo^{VI} [1,2,16,17], but other possible Mo valences cannot be categorically excluded. For instance, in the case of MoO_3/SiO_2 catalyst treated with tetramethyltin, Mo^{IV} surface alkylidene complex was proposed [18].

When investigating a reaction proceeding on a heterogeneous catalyst by quantum chemical methods, one of the main problems is modelling the infinite catalyst system. One approach to solve this problem is applying the cluster model [19–34]. This approach allows to perform minima and transition-state geometry optimisations and frequency calculations with using high-level theoretical methods. Therefore, it is particularly suited to tackle local phenomena, such as describing interactions of reactants with active sites of the catalyst [19–23,27–29,31,33–35]. Another problem is the choice of the optimal theoretical method. Such a method must be sufficiently accurate in describing electronic properties of the system, on the one hand, and the good computational efficiency should be guaranteed, on the other hand. Density functional theory methods satisfy these requirements, especially if systems containing transition metals are investigated [35–38].

In the previous work [39] density functional theory was applied to investigate ethene and propene metathesis reactions proceeding on monomeric Mo^{VI} and Mo^{IV} sites of MoO_3/Al_2O_3 catalyst. In the present work, more detailed study on ethene metathesis reaction proceeding on molybdenamethylidene centres of molybdena-alumina catalyst are reported. Thermodynamics of the elementary steps are calculated with applying the active sites models mounted on a small cluster of alumina. Its properties are compared with the properties of larger alumina clusters. To investigate the pathways of ethene addition to Mo^{VI} and Mo^{IV} methylidene centres (both singlet and triplet state), simpler models of the active sites, in which hydroxyl groups replace the bonds between molybdenum and the carrier, are applied.

2. Computational

Calculations were carried out with the Gaussian 94 program [40] installed on SPP1600/XA computer. The Slater local exchange functional and the VWN5

local correlation functional [41] were applied to optimise the geometries of the model clusters including alumina. The structures of the simpler models of the active sites were optimised with the B3LYP non-local functional [42] but in chosen cases SVWN5 method was used parallel. All the structures were optimised with applying Berny algorithm using redundant internal coordinates [43]. Harmonic vibration frequencies were calculated for each structure. The electronic energy of the structures was calculated using B3LYP functional. Three basis sets were employed: basis **A** — LANL2DZ basis set (the Hay–Wadt effective core potential [44] plus double-zeta basis for molybdenum and aluminium atoms, Dunning–Huzinaga valence double-zeta basis set — D95V [45] — for other non-transition elements), basis **B1** and **B2** — LANL2DZ basis set for molybdenum atom, D95V(d) and 6-31G(d) [45] basis set for non-transition elements, respectively.

Calculations of the alumina clusters alone were carried out with MOPAC 6 program using semiempirical AM1 Hamiltonian [46]. The clusters geometries were optimised using Bartel's method [47].

3. Results and discussion

3.1. Cluster models of alumina

A cluster model of Al_2O_3 with exposed fully hydroxylated (1 0 0) face (**A1**), developed by us, is shown in Fig. 1. It contains 24 aluminium atoms. The smaller alumina cluster (**A2**) with nine aluminium atoms and the third cluster (**A3**), containing only two aluminium atoms, are also presented in Fig. 1. In Table 1 the charges on the hydrogen and aluminium atoms and the deprotonation energies of the clusters are compared. The indexes "o" and "t" mean OH group
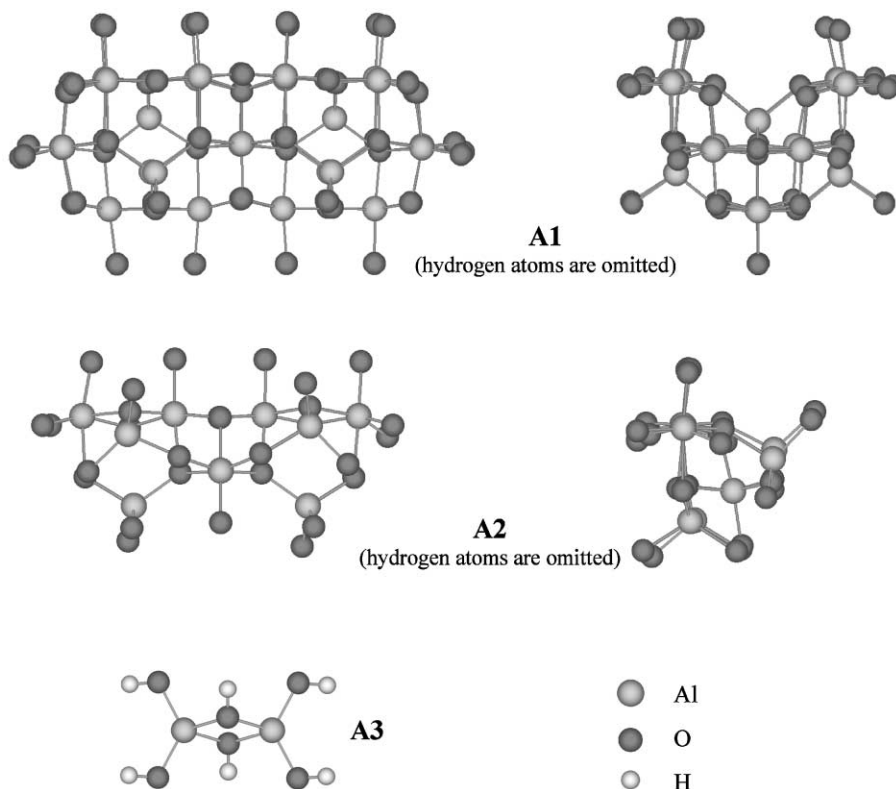

Fig. 1. Cluster models of alumina.

Table 1
Charges on hydrogen (q_H) and aluminium (q_{Al}) atoms and the deprotonation energies (E_d) for the model clusters of alumina

Structure	OH group	q_H	q_{Al}	E_d (kJ mol^{-1})
A1	OH^o	0.19–0.21	0.79–0.83	1300, 1330, 1410, 1420, 1440, 1470
	OH^t	0.22, 0.23	0.91–0.93	1200, 1220, 1240
	OH^{oo}	0.25, 0.26	–	1250
A2	OH^o	0.20, 0.21	0.80, 0.81	1410, 1420
	OH^{oo}	0.27	–	1230
A3	OH^t	0.21	0.83	1390
	OH^{tt}	0.28	–	1250

connected with octahedral and tetrahedral alumina centre, respectively. The deprotonation energy was defined as the energy difference between the cluster and its deprotonised form. The geometries of the deprotonised clusters were not further optimised, only the coordinates of the oxygen ion, remaining after proton abstraction, were optimised. The results shown in Table 1 indicate that the chemical properties of OH^t groups of the smallest cluster (**A3**) are reasonably similar to the properties of the OH^o groups of the two bigger clusters. Thus, the **A3** cluster can play the role of the carrier if one assumes that the Mo centres in molybdena-alumina catalyst replace hydroxyl groups connected with octahedral alumina.

3.2. Study on ethene addition to Mo^{VI} methylidene centres

Mo^{VI} complexes attached to the small alumina cluster are shown in Fig. 2. All the structures have C$_s$ symmetry. Four-coordinate Mo^{VI} methylidene centre (**1**) has pseudotetrahedral geometry. The TBP molybdacyclobutane (**2a**) has the almost flat ring, whereas the SP one (**2b**) has the ring with the dihedral angle of 27°. The thermodynamics of ethene addition to the Mo^{VI} methylidene centre (**1**) are presented in Table 2. SP molybdacyclobutane (**2b**) is predicted to be more stable than TBP structure (**2a**) by 38, 57 and 62 kJ mol^{-1} (ΔH°_{298}) according to B3LYP/A//SVWN5/A, B3LYP/B1//SVWN5/A and B3LYP/B2//SVWN5/A calculations, respectively. Therefore, the reaction leading to the SP molybdacyclobutane (**2b**) is thermodynamically favoured in comparison with the formation of the TBP molybdacyclobutane (**2a**). The formation of the former

structure is exothermic with relatively small absolute value of the change of Gibbs free energy (Table 2, entry II), whereas the latter reaction is clearly endoergic (Table 2, entry I).

Model structures of Mo^{VI} surface complexes, containing hydroxyl groups instead of the bonds between molybdenum and the carrier, are presented in Fig. 3. The C$_s$ geometries of the Mo^{VI} methylidene complex (**3**) and the molybdacyclobutanes (**7a**) and (**7b**) are very similar to the geometries of the respective complexes shown in Fig. 2. The SP molybdacyclobutane (**7b**) is predicted to be more stable than the TBP structure (**7a**). For instance, B3LYP/B1//SVWN5/A and B3LYP/B1 calculations give the energy difference ($T = 298.15$ K) of 64 and 66 kJ mol^{-1}, respectively. Comparing thermodynamics of reaction I and III or II and IV (Table 2), one can notice that the results obtained applying the simpler models of active centres are quite similar to those obtained for the clusters including alumina. Therefore, the reaction pathway of ethene addition to Mo^{VI} methylidene complex was investigated using the simpler models of the active sites. We can also state that the method of geometry optimisation scarcely influences the obtained energies of the complexes studied (Table 2, entries III and IV). Indeed, as it was also shown in the previous work [39], the optimised geometries of the active sites hardly depend on functional or basis set used.

The energy diagrams of the reaction are presented in Fig. 4. Structure (**5**) is the intermediate ethene-molybdenamethylidene complex with the Mo–C bond lengths of 2.74 and 2.79, and 1.37 Å of the C–C distance in ethene (Fig. 3). Sodupe et al. [12] reported quite similar geometry for ethene-tungsten-methylidene complex: 2.57 and 2.63,
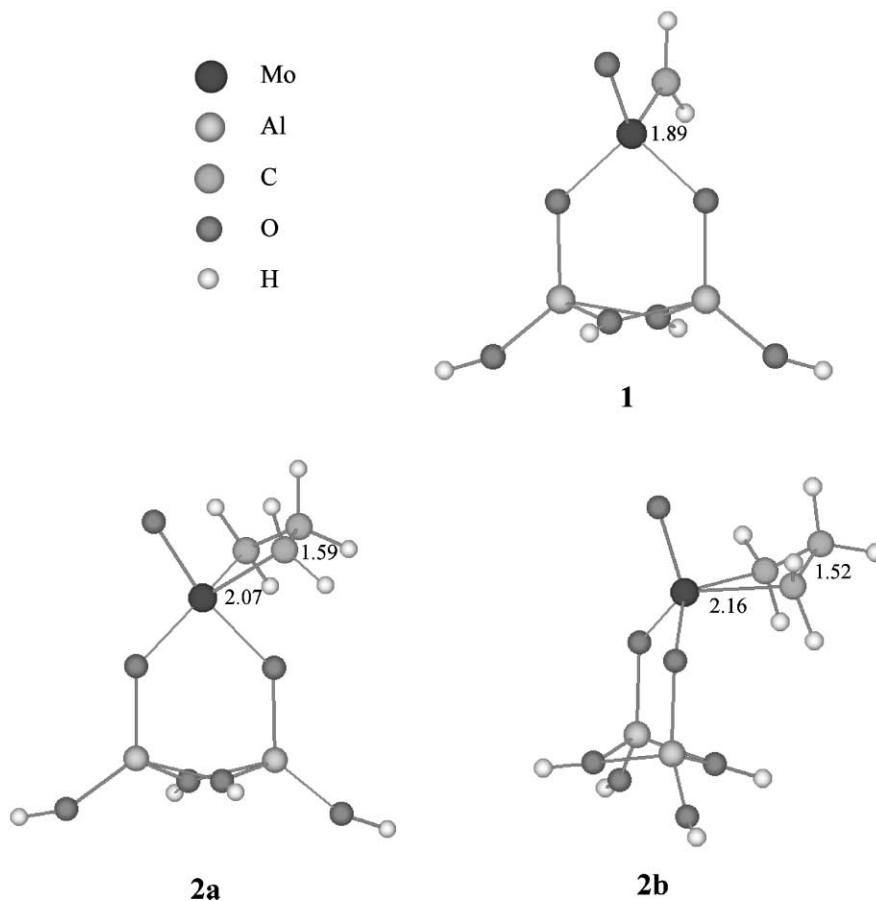
Fig. 2. Optimised structures of Mo^{VI} complexes including alumina. Bond lengths (in angstroms) are obtained from the SVWN5/A calculations.

and 1.37 Å for W–C and C–C bond lengths, respectively. According to their calculations, the complex of ethene with W(CH$_2$)Cl$_4$ is more stable than the reactants, while in the present work the formation of ethene-molybdenamethylidene complex (**5**) is predicted to be endothermic (Table 2, entry V). We have localised the transition state (**4**), which is situated between the reactants and the intermediate (**5**) — Fig. 3. As Table 2 and Fig. 4 show, the calculated activation enthalpy of the formation of the intermediate (**5**) is low: 18 and 15 kJ mol^{-1}, according to B3LYP/A and B3LYP/B1 calculations, respectively. The activation energy of the reverse reaction is very low (about 3 and 5 kJ mol^{-1}, using B3LYP/A and B3LYP/B1 method, respectively) if potential energy without the

zero point correction is taken into account (Fig. 4). However, the value of the calculated activation enthalpy at $T = 298.15$ K is negative (Fig. 4 and Table 2, entry VII).

The pathway of the rearrangement of the intermediate (**5**) to the TBP molybdacyclobutane passes through the transition state (**6**) — Figs. 3 and 4. The activation barrier of this step is lower than in the case of the previous step (Table 2, entry VIII). The activation enthalpy of the reverse step — the transformation of TBP molybdacyclobutane (**7a**) to the intermediate complex (**5**) — is also not high, with the value of about 33 and 27 kJ mol^{-1}, according to B3LYP/A and B3LYP/B1 calculations, respectively. However, this is the highest calculated energy barrier in the process.

Table 2
Calculated changes of enthalpies (ΔH°_{298}), Gibbs free energies (ΔG°_{298}) and entropies (ΔS°_{298}) for the reaction of Mo^{VI} centres[a]

Entry	Reaction	Method	ΔH°_{298} (kJ mol^{-1})	ΔG°_{298} (kJ mol^{-1})	ΔS°_{298} (J mol^{-1} K^{-1})
I	$1 + C_2H_4 \rightarrow 2a$	B3LYP/A//SVWN5/A	−4.8	50.0	−183.6
		B3LYP/B1//SVWN5/A	5.1	59.9	
		B3LYP/B2//SVWN5/A	−0.8	53.9	
II	$1 + C_2H_4 \rightarrow 2b$	B3LYP/A//SVWN5/A	−42.7	10.6	−178.7
		B3LYP/B1//SVWN5/A	−51.8	1.5	
		B3LYP/B2//SVWN5/A	−63.1	−9.8	
III	$3 + C_2H_4 \rightarrow 7a$	B3LYP/A//SVWN5/A	2.5	54.7	−175.3
		B3LYP/B1//SVWN5/A	−7.3	44.9	
		B3LYP/B2//SVWN5/A	−8.5	43.8	
		B3LYP/A	0.0	52.4	−175.9
		B3LYP/B1	−1.8	49.8	−173.0
		B3LYP/B2	−1.2	47.7	−164.0
IV	$3 + C_2H_4 \rightarrow 7b$	B3LYP/A//SVWN5/A	−56.5	−1.7	−183.6
		B3LYP/B1//SVWN5/A	−71.6	−16.8	
		B3LYP/B2//SVWN5/A	−75.0	−20.3	
		B3LYP/A	−58.8	−4.8	−181.2
		B3LYP/B1	−68.1	−14.3	−180.4
		B3LYP/B2	−70.1	−16.5	−179.8
V	$3 + C_2H_4 \rightarrow 5$	B3LYP/A	19.8	63.9	−148.0
		B3LYP/B1	15.4	60.7	−151.9
VI	$3 + C_2H_4 \rightarrow 4$ (TS)	B3LYP/A	18.2	59.1	−137.4
		B3LYP/B1	15.0	55.9	−137.0
VII	$5 \rightarrow 4$ (TS)	B3LYP/A	−1.6	−4.8	10.6
		B3LYP/B1	−0.4	−4.8	14.9
VIII	$5 \rightarrow 6$ (TS)	B3LYP/A	12.7	21.6	−30.1
		B3LYP/B1	10.0	19.1	−30.6
IX	$7a \rightarrow 6$ (TS)	B3LYP/A	32.5	33.1	−2.2
		B3LYP/B1	27.2	30.0	−9.5

[a] $T = 298.15$ K.

Reported experimental values of activation energy of propene metathesis carried out in the presence of heterogeneous catalysts containing rhenium or molybdenum are in the range of about 20–40 kJ mol^{-1} [48]. Thus, our theoretical calculations concerning ethene metathesis have given the value of the activation energy contained in this range.

The reaction and activation entropies of the reactants transformation to the intermediate (5) have high, negative values (Table 2, entries V and VI). This is why the respective Gibbs free energies have the large, positive values of about 60 kJ mol^{-1}. The Gibbs free energy of the overall reaction of ethene addition to the molybdenamethylidene complex (3) is about 50 kJ mol^{-1} (Table 2, entry III). However,

the predicted absolute values should be treated with caution, taking into consideration the simplicity of the models applied and the limited accuracy of the theoretical methods. Similar results concerning ethene addition to $Mo(NH)(CH_2)(OCH_3)_2$ complex have been obtained by Wu and Peng [15] using B3LYP functional, if Gibbs free energy of the reaction is calculated on the basis of the data reported by the authors.

Thermodynamics of ethene addition to the Mo^{VI} methylidene complex (3) leading to SP molybdacyclobutane (7b) do not much differ from the results obtained with applying active sites models including alumina (Table 2, entries II and IV). Reaction (IV) is exothermic and not very exoergic. However, we could
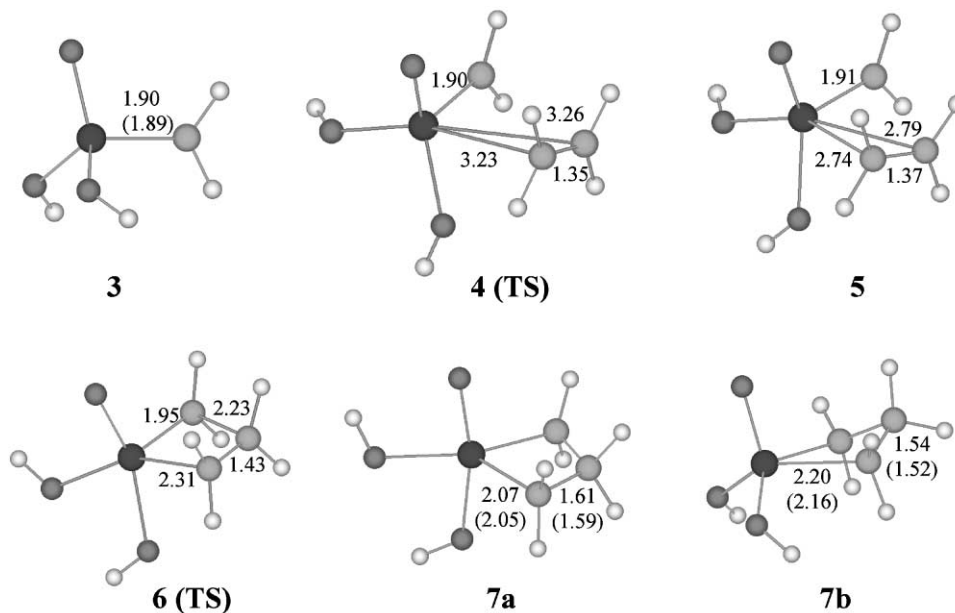
Fig. 3. Optimised structures of Mo[VI] complexes. Bond lengths (in angstroms) are obtained from the B3LYP/A and SVWN5/A (in parentheses) calculations.
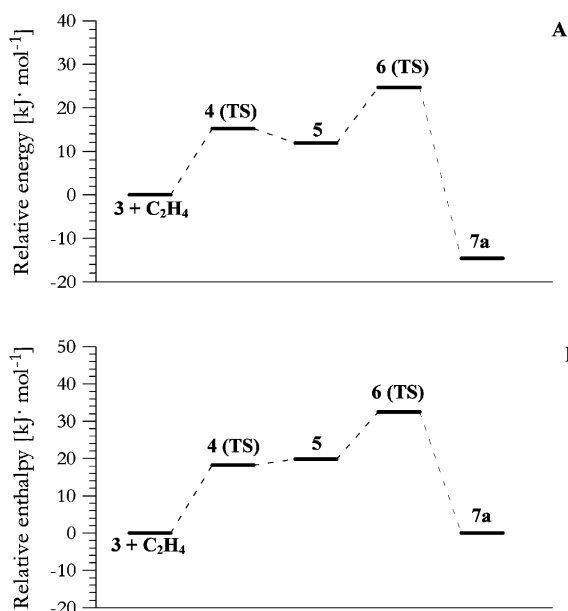

Fig. 4. Energy and enthalpy diagrams of ethene addition to Mo[VI] methylidene complex. B3LYP/A calculations. (A) Energy without the zero point energy including, (B) enthalpy at $T = 298.15$ K.

not find a transition structure connecting the reactants with the SP molybdacyclobutane (**7b**).

3.3. Study on ethene addition to Mo[IV] methylidene centres

Calculated structures of the Mo[IV] complexes, both models including alumina and the simpler models, are shown in Fig. 5 (singlet state) and in Fig. 6 (triplet state). As it was reported in the previous work [39], the complexes in triplet state have lower energies than the respective complexes in singlet state. The energy differences are shown in Table 3.

Table 3
Calculated differences between the enthalpies of the singlet state structures and the respective triplet state structures at $T = 298.15$ K

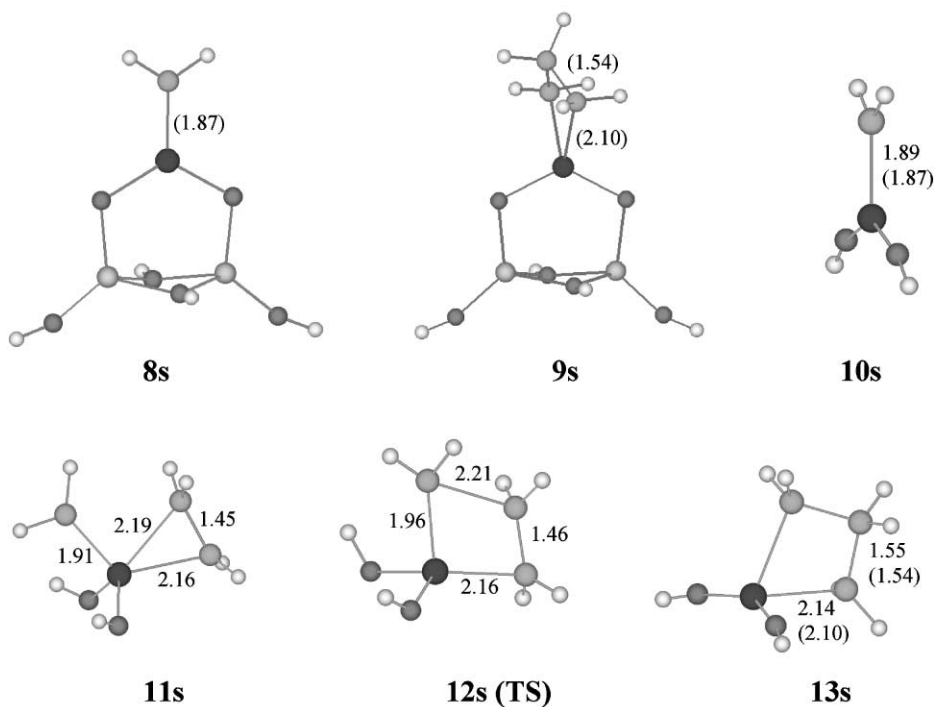| Structure	Method	ΔH°_{298} (kJ mol^{-1})
8	B3LYP/B1//SVWN5/A	16.8
9	B3LYP/B1//SVWN5/A	43.0
10	B3LYP/B1//SVWN5/A	36.6
	B3LYP/A	13.4
	B3LYP/B1	33.3
13	B3LYP/B1//SVWN5/A	56.6
	B3LYP/A	33.0

Fig. 5. Optimised structures of Mo^{IV} complexes (singlet state). Bond lengths (in angstroms) are obtained from the B3LYP/A and SVWN5/A (in parentheses) calculations.

Mo^{IV} methylidene complexes containing alumina (**8s**, **8t**) have C$_{2v}$ symmetry. The respective Mo^{IV} molybdacyclobutanes **9s** and **9t** have C$_s$ symmetry and their rings have dihedral angles of 21 and 37°, respectively. The geometries of the simpler models of Mo^{IV} centres: **10s**, **10t**, **13s**, **13t** are similar to the geometries of the models including alumina. The first structure has C$_{2v}$ symmetry, the last has no symmetry and the others have C$_s$ symmetry.

The thermodynamics of ethene addition to the Mo^{IV} methylidene centres are presented in Table 4 (singlet state) and Table 5 (triplet state). As we can see from Table 4 (entries X and XI), the overall reaction of ethene addition to Mo^{IV} centre (singlet state) leading to molybdacyclobutane formation is predicted to be high exothermic and exoergic. In the case of triplet state of Mo^{IV} centre, the process is even more exothermic and exoergic (Table 5, entries XV and XVI).

The results of the investigation of the reaction pathway of ethene addition to Mo^{IV} methylidene centre (singlet state) are shown in Figs. 5 and 7, and in Table 4. We have localised the additional ground state (**11s**) and the transition state (**12s**) connecting the (**11s**) complex and the molybdacyclobutane (**13s**). As comes from Table 4 (entry XII) and Fig. 7, the formation of the (**11s**) complex from the reactants is very exothermic and exoergic. However, both rearrangement of the (**11s**) complex to the molybdacyclobutane (**13s**) and the reverse reaction have high activation enthalpies and activation Gibbs free energies (about 100 kJ mol^{-1}, Table 4, entries XIII and XIV).

In the case of the reaction pathway of ethene addition to triplet state of the Mo^{IV} methylidene centre (Figs. 6 and 7), two additional ground states (**11ta** and **11tb**) have been localised. The reaction pathways of the formations of (**11ta**) and (**11tb**) are monotonic without transition states between the reactants and the products. Both reactions are moderately exothermic and endoergic (Table 5, entries XVII and XVIII).
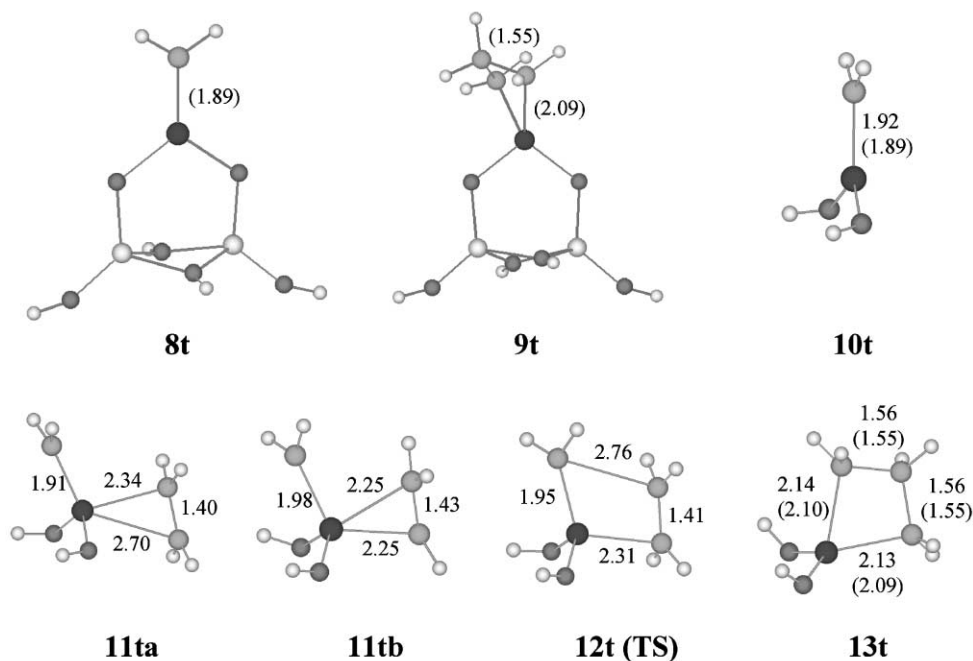
Fig. 6. Optimised structures of Mo^{IV} complexes (triplet state). Bond lengths (in angstroms) are obtained from the B3LYP/A and SVWN5/A (in parentheses) calculations.

Table 4
Calculated changes of enthalpies (ΔH°_{298}), Gibbs free energies (ΔG°_{298}) and entropies (ΔS°_{298}) for the reaction of Mo^{IV} complexes (singlet state)[a]

Entry	Reaction	Method	ΔH°_{298} (kJ mol^{-1})	ΔG°_{298} (kJ mol^{-1})	ΔS°_{298} (J mol^{-1} K^{-1})
X	**8s** + C$_2$H$_4$ → **9s**	B3LYP/A//SVWN5/A	−101.6	−45.6	−187.9
		B3LYP/B1//SVWN5/A	−108.6	−52.5	
		B3LYP/B2//SVWN5/A	−114.6	−58.6	
XI	**10s** + C$_2$H$_4$ → **13s**	B3LYP/B1//SVWN5/A	−112.6	−63.3	−165.4
		B3LYP/B2//SVWN5/A	−112.8	−63.5	
		B3LYP/A	−104.8	−56.1	−163.5
XII	**10s** + C$_2$H$_4$ → **11s**	B3LYP/A	−110.4	−60.2	−168.3
XIII	**11s** → **12s** (TS)	B3LYP/A	102.2	104.8	−8.6
XIV	**13s** → **12s** (TS)	B3LYP/A	96.6	100.6	−13.4

[a] $T = 298.15$ K.

However, we have found only one transition structure (**12t**), which is situated between the (**11tb**) intermediate and the molybdacyclobutane (**13t**). In this case, both activation enthalpy and activation Gibbs free energy are very low (Fig. 7 and Table 5, entry XIX). However, the reverse reaction has high activation enthalpy and activation Gibbs free energy (114 kJ mol^{-1} in both cases — Table 5, entry XX).

Therefore, as the above results (concerning both singlet and triplet state) show, it seems that the active sites of ethene metathesis do not contain Mo^{IV}, because the activation enthalpies of some elementary

Table 5
Calculated changes of enthalpies (ΔH°_{298}), Gibbs free energies (ΔG°_{298}) and entropies (ΔS°_{298}) for the reaction of Mo^{IV} complexes (triplet state)[a]

Entry	Reaction	Method	ΔH°_{298} (kJ mol^{-1})	ΔG°_{298} (kJ mol^{-1})	ΔS°_{298} (J mol^{-1} K^{-1})
XV	**8t** + C$_2$H$_4$ → **9t**	B3LYP/A//SVWN5/A	−125.8	−73.2	−176.5
		B3LYP/B1//SVWN5/A	−134.8	−82.2	
		B3LYP/B2//SVWN5/A	−135.4	−82.8	
XVI	**10t** + C$_2$H$_4$ → **13t**	B3LYP/B1//SVWN5/A	−132.6	−79.7	−165.4
		B3LYP/B2//SVWN5/A	−133.5	−80.6	
		B3LYP/A	−124.4	−74.0	−169.0
		B3LYP/B1	−134.4	−83.3	−171.3
XVII	**10t** + C$_2$H$_4$ → **11ta**	B3LYP/A	−21.9	20.9	−143.7
XVIII	**10t** + C$_2$H$_4$ → **11tb**	B3LYP/A	−15.3	31.0	−155.2
XIX	**11tb** → **12t** (TS)	B3LYP/A	5.4	8.7	−11.2
XX	**13t** → **12t** (TS)	B3LYP/A	114.4	113.7	2.6

[a] $T = 298.15$ K.

steps are much higher than the reported [48] experimental values of activation energies of olefin metathesis. We believe that this statement is true, even if the simplicity of the model applied and the limited accuracy of the theoretical methods are taken into account.
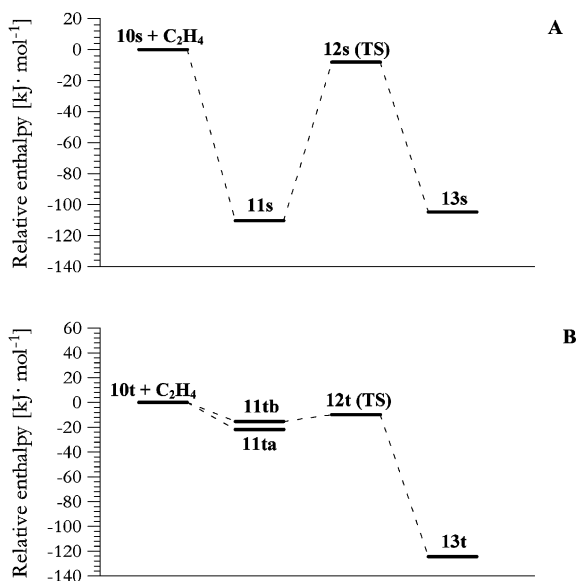

Fig. 7. Enthalpy diagrams ($T = 298.15$ K) of ethene addition to Mo^{IV} methylidene complex. (A) Singlet state; (B) triplet state B3LYP/A calculations.

4. Conclusions

Ethene metathesis proceeding on heterogeneous molybdena-alumina catalyst has been theoretically studied applying two variants of active sites models. In the first variant, the clusters contain alumina. In the second variant, the bonds between molybdenum and the carrier are replaced by hydroxyl groups. In both cases the calculated thermodynamics of ethene addition to molybdenamethylidene centres are very similar.

Investigation of reaction pathway of ethene addition to Mo^{VI} methylidene complex let us localise a transition state leading to TBP molybdacyclobutane. The formation of TBP molybdacyclobutane is an endoergic reaction with low activation enthalpy. Activation enthalpy of decomposition of TBP molybdacyclobutane to ethene and Mo^{VI} complex is a little higher and its value is consistent with the reported experimental values of activation energies of olefin metathesis. Ethene addition to Mo^{VI} methylidene complex leading to SP molybdacyclobutane is exothermic with small absolute value of reaction Gibbs free energy. However, we have not localised a transition structure leading to SP molybdacyclobutane.

On the other hand, energy barriers of one or two elementary steps (depending on consideration of singlet or triplet state of molybdenum complexes) of ethene metathesis proceeding on Mo^{IV} active sites are very high (over 100 kJ mol^{-1}). What is more, formation of the Mo^{IV} molybdacyclobutane is very exothermic and

irreversible. Therefore, the obtained results suggest that active centres of ethene metathesis do not contain Mo^{IV}.

Acknowledgements

References

[1] K.J. Ivin, J.C. Mol, Olefin Metathesis and Metathesis Polymerisation, Academic Press, London, 1997.

[2] J. Handzlik, J. Ogonowski, Metateza olefin, monografia, Politechnika Krakowska, seria Inzynieria i Technologia Chemiczna 223, Kraków, 1998.

[3] J.L. Herisson, Y. Chauvin, Makromol. Chem. 141 (1970) 161.

[4] A.K. Rappé, W.A. Goddard III, J. Am. Chem. Soc. 102 (1980) 5114.

[5] A.K. Rappé, W.A. Goddard III, J. Am. Chem. Soc. 104 (1982) 448.

[6] E.V. Anslyn, W.A. Goddard III, Organometallics 8 (1989) 1550.

[7] T.R. Cundari, M.S. Gordon, J. Am. Chem. Soc. 113 (1991) 5231.

[8] T.R. Cundari, M.S. Gordon, Organometallics 11 (1992) 55.

[9] L. Bencze, R. Szilagyi, J. Organom. Chem. 465 (1994) 211.

[10] L. Bencze, R. Szilagyi, J. Mol. Catal. 90 (1994) 157.

[11] L. Bencze, R. Szilagyi, J. Organom. Chem. 475 (1994) 183.

[12] M. Sodupe, J.M. Lluch, A. Oliva, J. Bertrán, J. Mol. Struct. (Theochem.) 251 (1991) 37.

[13] E. Folga, T. Ziegler, Organometallics 12 (1993) 325.

[14] H.H. Fox, M.H. Schofield, R.R. Schrock, Organometallics 13 (1994) 2804.

[15] Y.-D. Wu, Z.-H. Peng, J. Am. Chem. Soc. 119 (1997) 8043.

[16] K.A. Vikulov, I.V. Elev, B.N. Shelimov, V.B. Kazansky, J. Mol. Catal. 55 (1989) 126.

[17] W. Grünert, A.Yu. Stakheev, R. Feldhaus, K. Anders, E.S. Shpiro, K.M. Minachev, J. Catal. 135 (1992) 287.

[18] K. Tanaka, in: Y. Ímamoglu (Ed.), Olefin Metathesis and Polymerisation Catalysts, NATO ASI Series C326, Kluwer Academic Publishers, Dordrecht, 1990, p. 303.

[19] R.A. van Santen, J. Mol. Catal. A: Chemical 115 (1997) 405.

[20] M. Boronat, P. Viruela, A. Corma, J. Phys. Chem. A 102 (1998) 9863.

[21] E. Broclawik, Polish J. Chem. 72 (1998) 1551.

[22] M. Witko, K. Hermann, R. Tokarz, Catal. Today 50 (1999) 553.

[23] K. Hermann, M. Witko, A. Michalak, Catal. Today 50 (1999) 567.

[24] M. Witko, R. Tokarz, K. Hermann, Polish J. Chem. 72 (1998) 1565.

[25] A. Michalak, M. Witko, K. Hermann, Surf. Sci. 375 (1997) 385.

[26] K. Hermann, A. Michalak, M. Witko, Catal. Today 32 (1996) 321.

[27] E. Broclawik, R. Yamauchi, A. Endou, M. Kubo, A. Miyamoto, J. Chem. Phys. 104 (1996) 4098.

[28] E. Broclawik, H. Himei, M. Yamadaya, M. Kubo, A. Miyamoto, R. Vetrivel, J. Chem. Phys. 103 (1995) 2102.

[29] H. Himei, M. Yamadaya, M. Kubo, R. Vetrivel, E. Broclawik, A. Miyamoto, J. Phys. Chem. 99 (1995) 12461.

[30] E. Broclawik, J. Datka, B. Gil, J. Mol. Catal. 82 (1993) 347.

[31] A.M. Rigby, G.J. Kramer, R.A. van Santen, J. Catal. 170 (1997) 1.

[32] P. Faye, E. Payen, D. Bougeard, J. Catal. 179 (1998) 560.

[33] R.M. Watwe, B.E. Spiewak, R.D. Cortright, J.A. Dumesic, J. Catal. 180 (1998) 184.

[34] R.A. van Santen, G.J. Kramer, Chem. Rev. 95 (1995) 637.

[35] J.W. Andzelm, A.E. Alvarado-Swaisgood, F.U. Axe, M.W. Doyle, G. Fitzgerald, C.M. Freeman, A.M. Gorman, J.-R. Hill, C.M. Kölmel, S.M. Levine, P.W. Saxe, K. Stark, L. Subramanian, M.A. van Daelen, E. Wimmer, J.M. Newsam, Catal. Today 50 (1999) 451.

[36] T. Ziegler, Chem. Rev. 91 (1991) 651.

[37] T. Ziegler, Pure Appl. Chem. 63 (1991) 873.

[38] T. Ziegler, Can. J. Chem. 73 (1995) 743.

[39] J. Handzlik, J. Ogonowski, Stud. Surf. Sci. Catal. 130 (2000) 1181.

[40] M.J. Frisch, G.W. Trucks, H.B. Schlegel, P.M.W. Gill, B.G. Johnson, M.A. Robb, J.R. Cheeseman, T.A. Keith, G.A. Petersson, J.A. Montgomery, K. Raghavachari, M.A. Al-Laham, V.G. Zakrzewski, J.V. Ortiz, J.B. Foresman, J. Cioslowski, B.B. Stefanov, A. Nanayakkara, M. Challacombe, C.Y. Peng, P.Y. Ayala, W. Chen, M.W. Wong, J.L. Andres, E.S. Replogle, R. Gomperts, R.L. Martin, D.J. Fox, J.S. Binkley, D.J. Defrees, J. Baker, J.P. Stewart, M. Head-Gordon, C. Gonzalez, J.A. Pople, Gaussian 94, Revision E.1, Gaussian Inc., Pittsburgh, PA, 1995.

[41] S.H. Vosco, L. Wilk, M. Nusair, Can. J. Phys. 58 (1980) 1200.

[42] A.D. Becke, J. Chem. Phys. 98 (1993) 5648.

[43] C. Peng, P.Y. Ayala, H.B. Schlegel, M.J. Frisch, J. Comp. Chem. 17 (1996) 49.

[44] P.J. Hay, W.R. Wadt, J. Chem. Phys. 82 (1985) 299.

[45] M.J. Frisch, E. Frisch, J.B. Foresman, Gaussian 94 User's Reference, Gaussian Inc., Pittsburgh, PA, 1996.

[46] M.J.S. Dewar, E.G. Zoebisch, E.F. Healy, J.P. Stewart, J. Am. Chem. Soc. 107 (1985) 3902.

[47] M.B. Coolidge, J.J.P. Stewart, MOPAC Manual, 6th Edition, 1990.

[48] F. Kapteijn, H.L.G. Bredt, E. Homburg, J.C. Mol, Ind. Eng. Chem. Prod. Res. Dev. 20 (1981) 457.